PRP Pharmacology Research & Perspectives
Open Access

ORIGINAL ARTICLE

VGF and striatal cell damage in in vitro and in vivo models of Huntington's disease

Yasuhiro Noda[1], Masamitsu Shimazawa[1], Hirotaka Tanaka[1], Shigeki Tamura[2], Teruyoshi Inoue[2], Kazuhiro Tsuruma[1] & Hideaki Hara[1]

[1]Molecular Pharmacology, Department of Biofunctional Evaluation, Gifu Pharmaceutical University, 1-25-4 Daigaku-nishi, Gifu 501-1196, Japan
[2]Asubio Pharma Co., Ltd., 6-4-3, Minatojima-Minamimachi, Chuo-ku, Kobe 650-0047, Japan

Keywords
AQEE-30, Huntington's disease, neuroprotection, SUN N8075, VGF

Correspondence
Hideaki Hara, Molecular Pharmacology, Department of Biofunctional Evaluation, Gifu Pharmaceutical University, 1-25-4 Daigaku-nishi, Gifu 501-1196, Japan.
Tel/Fax: +81-58-230-8126;
E-mail: hidehara@gifu-pu.ac.jp

Funding Information
This study was supported in a research grant and providing SUN N8075 by Asubio Pharma Co., Ltd. ST and TI are employees of Asubio Pharma.

Received: 19 August 2014; Revised: 4 March 2015; Accepted: 10 March 2015

Pharma Res Per, 3(3), 2015, e00140, doi: 10.1002/prp2.140

doi: 10.1002/prp2.140

Abstract

Huntington's disease (HD) is an inherited genetic disorder, characterized by cognitive dysfunction and abnormal body movements, and at present there is no effective treatment for HD. Therapeutic options for HD are limited to symptomatic treatment approaches and there is no cure for this devastating disease. Here, we examined whether SUN N8075, (2*S*)-1-(4-amino-2,3,5-trimethylphenoxy)-3-{4-[4-(4-fluorobenzyl)phenyl]-1-piperazinyl}-2-propanol dimethanesulfonate, which exerts neuroprotective effects by antioxidant effects and induction of VGF nerve growth factor inducible (VGF), has beneficial effects in STHdh cells derived from striatum of knock-in HD mice and R6/2 HD mice. In an in vitro study, SUN N8075 inhibited the cell death caused by mutant huntingtin (mHtt) and upregulated the *VGF* mRNA level via the phosphorylation of extracellular signal-regulated kinase 1/2 (ERK1/2). Furthermore, 30 amino acid of VGF C-terminal peptide, AQEE-30 inhibited the cell death and the aggregation of mHtt. In an in vivo study, SUN N8075 improved the survival and the clasping response in the R6/2 mice. Furthermore, SUN N8075 increased the number of surviving neurons in the striatum of the R6/2 mice. These findings suggest that SUN N8075 may be an effective candidate for HD treatments.

Abbreviations

ALS, amyotrophic lateral sclerosis; BDNF, brain-derived neurotrophic factor; DMEM, Dulbecco's modified Eagle's medium; DMSO, dimethylsulfoxide; ERK1/2, extracellular signal-regulated kinase 1/2; ER-stress, endoplasmic reticulum stress; FBS, fetal bovine serum; HD, Huntington's disease; MAPKK, mitogen-activated protein kinase kinase; MEK, mitogen-activated protein kinase/ERK kinase; mHtt, mutant huntingtin; MSNs, medium spiny neurons; PBS, phosphate-buffered saline; PI, propidium iodide; PVDF, polyvinylidene difluoride; SDS, sodium dodecyl sulfate; VGF, VGF nerve growth factor inducible; WT, wild-type.

Introduction

Huntington's disease (HD) is a hereditary neurodegenerative disease that is caused by a mutation in the gene coding for a ubiquitously expressed protein, huntingtin (Htt) (Rubinsztein 2002). Mutant Htt (mHtt) causes the death of neurons via its aggregation, particularly in medium spiny neurons (MSNs), the phenotype that accounts for 90% of striatal neurons. The demise of MSNs causes dysfunctional motor, cognitive and behavioral symptoms (Reiner et al. 1988). One possible mechanism of neuronal degeneration in HD is a reduction in neurotrophic factor activity (Zuccato et al. 2001). However, the underlying mechanisms of neurodegeneration and mHtt aggregation are not well understood, and at present, there are no effective treatments for HD. Therefore, therapeutic options for HD are limited to symptomatic approaches and there is no cure yet in sight for this devastating disease. In our recent studies, we examined a novel agent against neuronal degeneration, SUN N8075 [(2*S*)-1-(4-

amino-2,3,5-trimethylphenoxy)-3-{4-[4-(4-fluorobenzyl) phenyl]-1-piperazinyl}-2-propanol dimethanesulfonate], which was synthesized as an inhibitor for Na^+ and T-type Ca^{2+} channels with a potent antioxidative effect (Annoura et al. 2000). Our previous studies revealed potent neuroprotective activities of this agent in an in vivo transient middle cerebral artery occlusion model (Kotani et al. 2007), Parkinson's disease (Oyagi et al. 2008), retinal damage induced by intravitreous injection of *N*-methyl-D-aspartate or high-intraocular pressure (Akane et al. 2011), and amyotrophic lateral sclerosis (ALS) (Shimazawa et al. 2010). These neuroprotective effects were the result of multiple mechanisms such as the compound's antioxidant activity (Kotani et al. 2007; Oyagi et al. 2008; Akane et al. 2011) and the upregulation of VGF nerve growth factor inducible (VGF) (Shimazawa et al. 2010). However, the neuroprotective effects of SUN N8075 have not yet been studied in HD. In the present study, we examined whether SUN N8075 inhibited the cell death of STHdhQ111 cells, a model of HD by aggregation of mHtt. Furthermore, we investigated the effects of SUN N8075 on the survival, motor performance, and suppression of striatal neuronal degeneration in R6/2 model mice.

Materials and Methods

Cell lines

The striatally derived cell lines, STHdhQ7 and STHdhQ111, were purchased from Coriell Institute for Medical Research (Camden, NJ). These cell lines were established from striatal precursors obtained from E14 mouse embryos that expressed either Htt with 7 polyQ or mHtt with 111 polyQ. Cells were grown in Dulbecco's modified Eagle's medium (DMEM; Sigma-Aldrich, St. Louis, MO) containing 10% fetal bovine serum (FBS; Valeant, Costa Mesa, CA) at 33°C with 5% CO_2. Because various stresses such as ER-stress and oxidative stress contribute to the pathology of HD (Browne et al. 1997; Reijonen et al. 2008), we performed the in vitro experiments under conditions of starvation stress.

Cell death assay

To evaluate the effects of SUN N8075 on cell death induced by aggregation of mHtt, both STHdhQ7 and Q111 cells were seeded at a density of 5×10^3 cells per well into 96-well plates, and then incubated in a humidified atmosphere of 95% air and 5% CO_2 at 33°C for 24 h. SUN N8075 was dissolved in dimethylsulfoxide (DMSO; Nacalai Tesque Inc., Kyoto, Japan) and diluted with phosphate-buffered saline (PBS) containing 1% DMSO, after which it was added to the wells at final concentrations of 0.1, 0.3, 1, and 3 μmol/L upon replacing the medium with DMEM or DMEM containing 3% FBS. We also evaluated the effects of VGF peptide on STHdhQ111 cells, by adding 30 amino acids of the rat VGF C-terminal peptide AQEE-30 (Medical & Biological Laboratories Co., Ltd, Aichi, Japan) and 21 amino acids of the rat VGF peptide TLQP-21 (R&D Systems, Inc., MN, USA) after dissolving in PBS. In the experiment using MEK inhibitors, U0126 (Promega Corporation, WI, USA) and PD184352 (Sigma), SUN N8075 and MEK inhibitor were added together. U0126 and PD184352 were dissolved in DMSO and diluted with 1% DMSO PBS (at final concentration of 10 μmol/L). Cell viability was measured 12 h after treatment with SUN N8075. At the end of cultivation, Hoechst 33342 (Molecular Probes, OR) and propidium iodide (PI) (Zuccato et al. 2001) (Molecular Probes, OR, USA) were added to the culture medium for 15 min. Hoechst 33342 freely enters living cells and cells that have suffered apoptosis or necrosis. PI is a membrane-impermeant dye that is generally excluded from viable cells. Images were collected using a digital camera (COOLPIX 4500; Nikon, Tokyo, Japan). We used an image-processing software (Image-J ver. 1.33f; National Institutes of Health, Bethesda, MD) for cell counting.

Western blot analysis

STHdh cells were washed with PBS, harvested, and lysed using RIPA buffer (R0278; Sigma) with protease (P8340; Sigma) and phosphatase inhibitor cocktails (P2850 and P5726; Sigma). Lysates were solubilized in sodium dodecyl sulphate (SDS) sample buffer, separated on 10% SDS-polyacrylamide gels, and transferred to polyvinylidene difluoride (PVDF) membranes (Immobilon-P; EMD Millipore Corporation, Billerica, MA). Transfer membranes were blocked for 30 min at room temperature with Blocking One-P (Nakalai Tesque, Kyoto, Japan), then incubated overnight at 4°C with the primary antibodies (rabbit anti-phospho-extracellular signal-regulated kinase 1/2 [ERK1/2] [Cell Signaling Technology, Danvers, MA], rabbit anti-total-ERK1/2 [Cell Signaling Technology], and mouse anti-β-actin [Sigma]). Subsequently, the membranes were incubated with secondary antibodies (peroxidase-conjugated goat anti-rabbit IgG [Thermo Fisher Scientific Inc., Franklin, MA] or peroxidase-conjugated goat anti-mouse antibody [Thermo]). The immunoreactive bands were visualized using ImmnoStar®LD (Wako Pure Chemical Industries, Osaka, Japan) and the LAS-4000 Luminescent Image Analyzer (Fuji Film Co., Ltd., Tokyo, Japan).

Real-time RT-PCR

To evaluate the effect of SUN N8075 on the expression of *Vgf* mRNA, STHdhQ7, and Q111 cells were seeded in 24-well plates at a density of 2.5×10^4 cells per well. After cultivation for 24 h, the cells were incubated in 3% FBS DMEM or DMEM (serum free) and treated with 3 μmol/L SUN N8075 for 6 h. In the experiment using U0126, SUN N8075 and U0126 were simultaneously added to the cells. RNA extraction was performed using NucleoSpin® RNA II (Takara Bio Inc., Shiga, Japan). Quantitative real-time RT-PCR was performed using a Thermal Cycler Real Time System (TP-800; Takara Bio Inc.) with a SYBR® *Premix Ex Taq*™ II (Takara Bio Inc.), according to the manufacturer's protocol. The primers used for amplification were as follows: *Vgf* mRNA, 5′-GGCTGTTCTATTTA ATCGTCTGAAG-3′ (forward), and 5′-GGGTAAGTTCA CAGCAATTTGGA-3′ (reverse); *GAPDH* (glyceraldehyde-3-phosphate dehydrogenase) mRNA, 5′-TGTGTCCGTCG TGGATCTGA-3′ (forward) and 5′-TTGCTGTTGAAGTC GCAGGAG-3′ (reverse). The results are expressed relative to the GAPDH internal control.

Fluorescence immunostaining

STHdh cells were incubated in the Lab-Tek II Chamber Slide system (Thermo) for 24 h, and then treated with SUN N8075 and AQEE-30. After 12 h of treatment, the cells were washed with PBS, fixed in 4% paraformaldehyde for 15 min at room temperature, and permeabilized with 0.2% Triton X-100 for 10 min. Cells were incubated in 3% normal goat serum for 30 min and then incubated in Can Get Signal® Immunostain solution A (Toyobo Co., Ltd., Osaka, Japan) containing anti-huntingtin monoclonal antibody, clone 4A4.2 (EMD Millipore Corporation) at 4°C overnight. Next, the cells were washed with PBS and incubated at room temperature with Alexa Fluor 488 rabbit anti-mouse antibody (1:1000 dilution; Molecular Probes) for 1 h, and then incubated with Hoechst 33342 (1:1000) in PBS for 5 min. Huntingtin aggregates were viewed with a confocal microscope (FV10i, Olympus, Tokyo, Japan). The percentage of cells that contained aggregates within each group was determined.

Study animals

Transgenic male and female R6/2 mice (B6CBA-TgN [HDexon1]62Gpb) were purchased from the Jackson Laboratory (Bar Harbor, ME). The R6/2 line is characterized by a rapidly progressive HD phenotype that leads to death in 13–14 weeks (Mangiarini et al. 1996). We carefully observed the development of HD symptoms and identified symptomatic disease onset as when the mice showed clasping behavior. All mice were housed in a room under lighting conditions of 12-h light and 12-h dark.

Animal welfare and ethical statements

All experiments were approved and monitored by the Institutional Animal Care and Use Committee of Gifu Pharmaceutical University.

Drugs

We have previously reported that SUN N8075 exerted the beneficial effects on the model mice of neurodegenerative disease such as Parkinson's disease and ALS (Oyagi et al. 2008). Therefore, in this study, we performed the experiment in equivalent doses. SUN N8075 was dissolved in 6% Captisol solution, and subcutaneously administered at doses of 30 mg/kg, once daily from 4 weeks of age until the end of the animals' lives. In the control group, vehicle (6% Captisol solution) was subcutaneously administered at 10 mL/kg.

Survival

Mortality was scored as the day when the mouse was unable to right itself within 30 s after being placed on its back.

Rotarod test

Mice were tested for their ability to maintain balance on a rod (3 cm diameter) rotating at 5 rpm on a rotarod apparatus (Bio-Medica Ltd, Osaka, Japan). To adapt the mice to the apparatus, they were allowed to adjust to balancing on the rod as it rotated (5 rpm) for 7 days from when they were 21 days old. After this period of adaptation, locomotor performance was evaluated as the rod rotated at 5 rpm starting at 28 days of age. Testing was conducted two times per week until the animals became moribund. Each session consisted of three trials (10 min/trial). Performance time for each trial was recorded as the longest time the mice could stay on the rod without falling.

Clasping performance

An analysis of clasping was performed by suspending the mice from their tails at least 1 foot above a surface for 1 min, as previously described by Baquet et al. (2004).

Tissue processing

At 10 weeks of age, mice were anesthetized with sodium pentobarbital (80 mg/kg; i.p.; Nacalai Tesque Inc.) and

perfused with 2% paraformaldehyde solution, after which their brains were immersed in the same fixative solution for 24 h. After fixation, the brains were soaked in 25% (w/v) sucrose at 4°C for 1 day, and then frozen in embedding compound (Tissue-Tek; Sakura Finetechnical Co. Ltd., Tokyo, Japan). Coronal sections (Bregma + 0.14 mm) were stained with cresyl violet (Sigma).

Data analysis and statistical procedures

Data were presented as means ± SEM. Statistical comparisons were made by way of a Tukey's test, or Dunnett's test, or Student's *t*-test. Statistical analysis of the mean age of clasping and survival was performed with a log-rank test. $P < 0.05$ was considered to indicate statistical significance.

Results

SUN N8075 inhibited cell death in STHdh cells

We investigated the effects of SUN N8075 on cell death caused by the aggregation of mHtt in STHdhQ111 cells. STHdhQ7 cells, which express normal Htt, were used as a control.

Representative fluorescence images of Hoechst 33342 and PI staining are shown in Figure 1A. Cell death

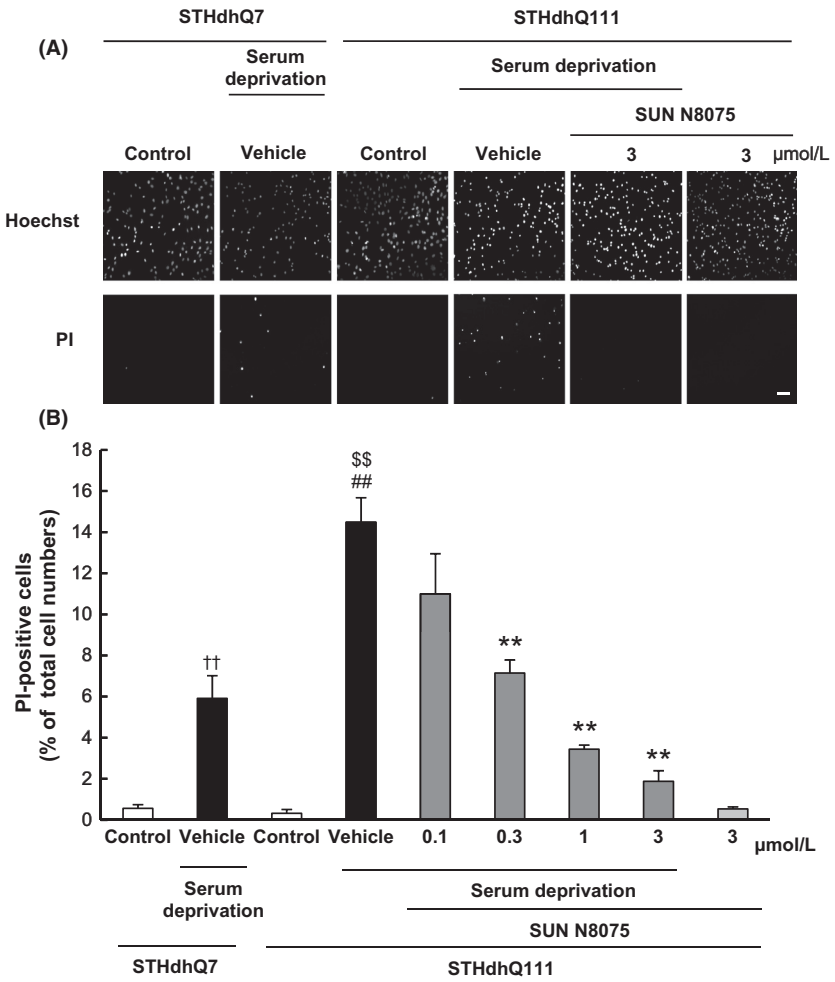

Figure 1. The effects of SUN N8075 on STHdh cell survival. (A) Representative fluorescence microscopic image of Hoechst 33342 and propidium iodide (PI) (Zuccato et al. 2001) staining. Scale bar represents 100 μm. (B) The number of cells exhibiting PI fluorescence was counted, and positive cells were expressed as the percentage of PI-positive to Hoechst 33342-positive cells. SUN N8075 treatment significantly decreased PI-positive cells. Values are mean ± SEM ($n = 5$). $^{**}P < 0.01$ versus vehicle group in STHdhQ111 (Dunnett's test), $^{\#\#}P < 0.01$ versus vehicle group in STHdhQ7 (Student's *t*-test), $^{\dagger\dagger}P < 0.01$ versus control group in STHdhQ7 (Student's *t*-test), $^{\$\$}P < 0.01$ versus control group in STHdhQ111 (Student's *t*-test). In all in vitro study, *n* represents the number of well.

observed in both STHdhQ7 and Q111 cells was significantly increased under the starvation stress condition compared with each control group (Fig. 1B). Furthermore, cell death in vehicle-treated STHdhQ111 cells was significantly increased compared with vehicle-treated STHdhQ7 cells (Fig. 1B). Notably, SUN N8075 significantly inhibited cell death in STHdhQ111 cells at concentrations of 0.3–3 μmol/L, with the most prominent effects observed at 3 μmol/L (Fig. 1B).

SUN N8075 upregulated the phosphorylation of ERK1/2

To confirm the mechanism by which SUN N8075 mediates its neuroprotective effects, we examined the effects of SUN N8075 treatment on levels of phospho-ERK1/2 (p-ERK1/2), a molecule known to be involved in signaling pathways that modulate cell survival. Western blot analysis results showed that SUN N8075 upregulated p-ERK1/2 levels in STHdhQ111 cells as early as 1 h after treatment (Fig. 2B). Furthermore, p-ERK1/2 levels were significantly decreased in STHdhQ111 cells under the starvation stress condition, and SUN N8075 significantly suppressed the downregulation of p-ERK1/2 1 h after treatment (Fig. 2C and D).

SUN N8075 upregulation of *Vgf* mRNA and VGF peptide expression exerted protective effects in STHdhQ111 cells

We have previously reported that SUN N8075 increased VGF, a neuropeptide with neuroprotective effects against endoplasmic reticulum stress (ER-stress) (Shimazawa et al. 2010). To confirm whether SUN N8075 induced VGF expression in STHdh cells, we performed quantitative RT-PCR. In STHdhQ111 cells, *Vgf* mRNA levels were significantly decreased in the serum-deprived condition; however, treatment with SUN N8075 significantly suppressed the downregulation of *Vgf* mRNA level 6 h after treatment (Fig. 3A). Furthermore, we performed a cell death assay to confirm whether VGF has neuroprotective effects in STHdhQ111 cells. A schematic diagram of the rat VGF precursor protein and processed peptides is shown in Figure 3B. The VGF peptide AQEE-30 significantly inhibited STHdhQ111 cell death at concentrations from 0.3–3 μmol/L (Fig. 3C); however, no effects

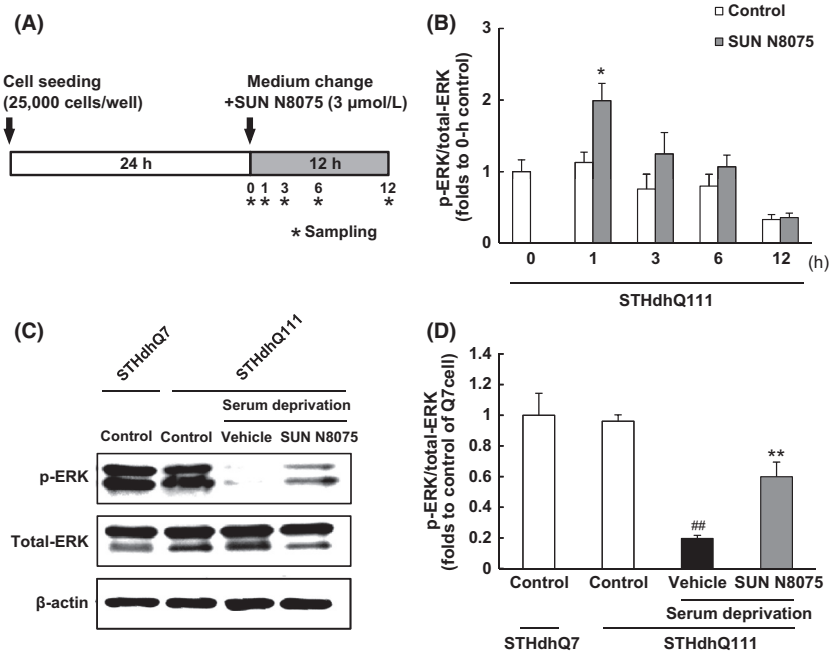

Figure 2. The effects of SUN N8075 on phosphorylation of extracellular signal-regulated kinase1/2 (ERK1/2). SUN N8075 treatment increased phosphorylated ERK1/2 (p-ERK1/2) in STHdh cells. (A) Schematic depiction of the experiment in Fig. 2A. (B) Time-dependent change in p-ERK1/2 expression level was assessed by western blotting. Treatment with SUN N8075 (3 μmol/L) upregulated the phosphorylation of ERK1/2 1 h after treatment. *$P < 0.05$ versus 1 h control group in STHdhQ111 (Student's *t*-test). (C) Membranes showing the immunoreactive bands of ERK1/2. (D) p-ERK1/2 expression was significantly increased 1 h after treatment with SUN N8075 (3 μmol/L) under the starvation stress condition. Values are mean ± SEM ($n = 4$). ##$P < 0.01$ versus control group in STHdhQ111 (Student's *t*-test), **$P < 0.01$ versus vehicle group in STHdhQ111 (Student's *t*-test). ERK1/2, extracellular signal-regulated kinase 1/2.

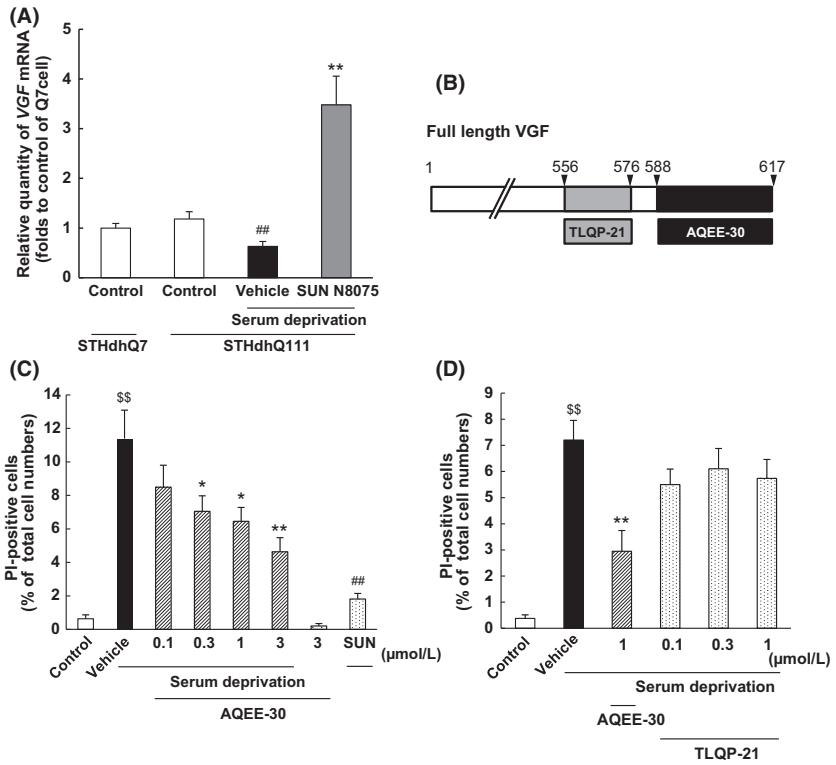

Figure 3. The effects of SUN N8075 on *Vgf* mRNA expression and neuroprotective effects of VGF peptides. (A) Schematic depiction of the rat VGF precursor protein and peptides. (B) The graph shows the relative quantity of *Vgf* mRNA (folds to control of STHdhQ7 cells). The *Vgf* mRNA level in STHdhQ111 cells was significantly increased 6 h after treatment with SUN N8075 (3 μmol/L). Values are mean ± SEM (n = 4). $^{\#\#}P < 0.01$ versus control group in STHdhQ111 (Student's *t*-test), $^{**}P < 0.01$ versus vehicle group in STHdhQ111 (Student's *t*-test). (C) The number of cells exhibiting PI fluorescence was counted, and positive cells were expressed as the percentage of PI-positive to Hoechst 33342-positive cells. Treatment with AQEE-30 significantly decreased the number of PI-positive cells. SUN, 3 μmol/L SUN N8075. Values are mean ± SEM (n = 6). $^{*}P < 0.05$ versus vehicle group (Dunnett's test), $^{**}P < 0.01$ versus vehicle group (Dunnett's test), $^{\#\#}P < 0.01$ versus vehicle group (Student's *t*-test), $^{\$\$}P < 0.01$ versus control group (Student's *t*-test). (D) The number of cells exhibiting PI fluorescence was counted, and positive cells were expressed as the percentage of PI-positive to Hoechst 33342-positive cells. TLQP-21 exerted no effects on cell death of STHdhQ111 cells. Values are mean ± SEM (n = 4). $^{\$\$}P < 0.01$ versus control group (Student's *t*-test), $^{**}P < 0.01$ versus vehicle group (Student's *t*-test). PI, propidium iodide; VGF, VGF nerve growth factor inducible.

were observed with the second VGF peptide tested, TLQP-21 (Fig. 3D).

SUN N8075 and AQEE-30 inhibited the aggregation of mHtt

To evaluate the effects of SUN N8075 and VGF peptides on the aggregation of mHtt, we performed fluorescence immunostaining. Representative fluorescence images are shown in Figure 4A, and the percentage of cells that included the aggregates was determined (Fig. 4B). In the nontreated group, there were some aggregates in STHdhQ111 cells (Fig. 4A). On the other hand, in the groups which treated with SUN N8075 and AQEE-30, aggregates of mHtt were significantly decreased (Fig. 4B).

MEK inhibitor suppressed the upregulation of *Vgf* mRNA and neuroprotective effects induced by SUN N8075

VGF is upregulated through mitogen-activated protein kinase kinase (MAPKK) and its target ERK (MEK/ERK) signaling pathway (Monteggia et al. 2004; Duman and Monteggia 2006; Adachi et al. 2008). Based on the results depicted in Figures 2, 3 of the present reports, we proposed the hypothesis that the upregulation of *Vgf* mRNA and improved cell viability caused by SUN N8075 treatment may be suppressed by inhibition of ERK activation. To confirm this hypothesis, we performed RT-PCR and cell death assay using the MEK inhibitors U0126 and PD184352. Treatment of STHdhQ111 cells with U0126 significantly suppressed the upregulation of *Vgf* mRNA

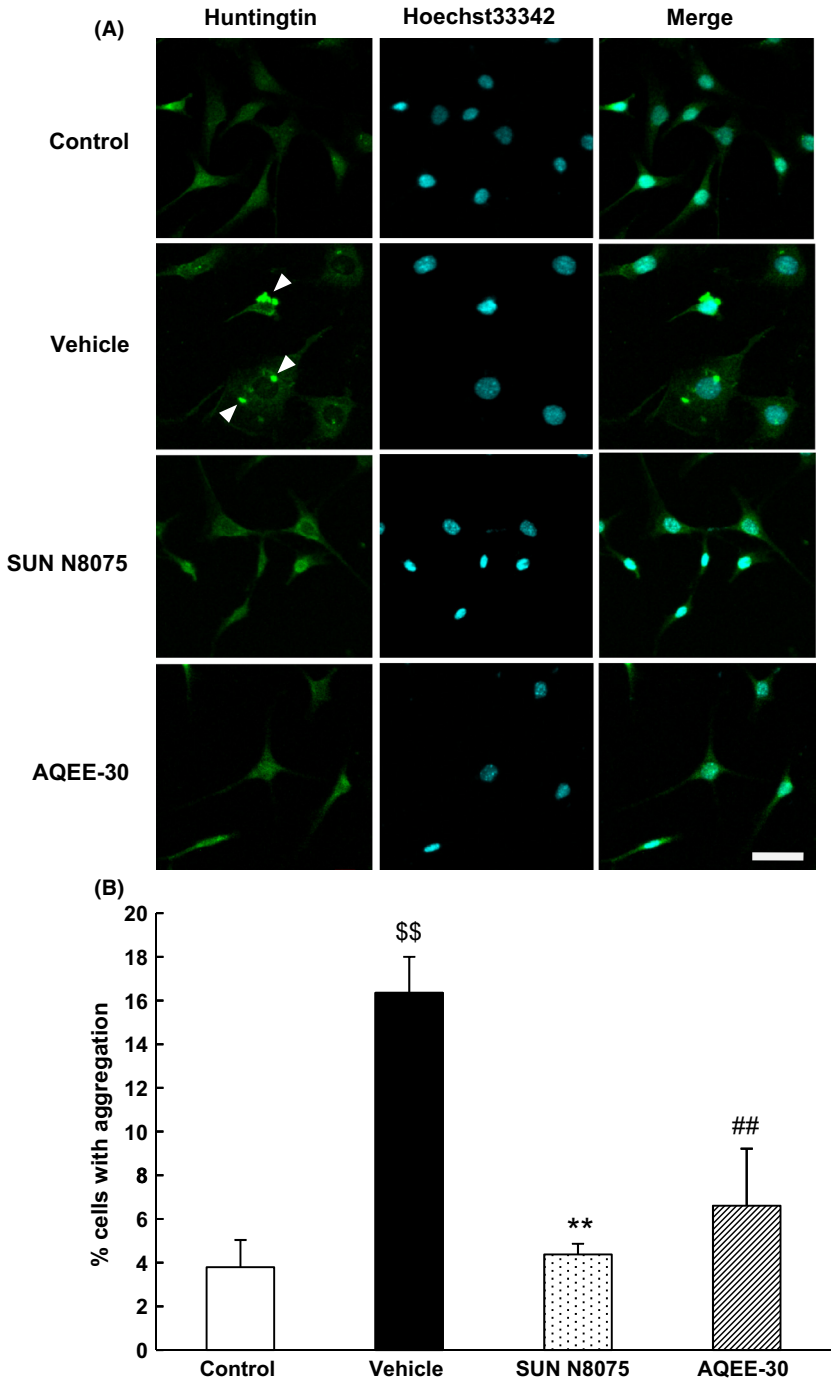

Figure 4. SUN N8075 and AQEE-30 inhibited the aggregation of mutant huntingtin. (A) Images of confocal microscopy are shown. (B) The percentage of cells that include the aggregates to whole cells. Serum deprivation increased aggregation of mHtt in STHdhQ111 cells. In contrast, SUN N8075 and AQEE-30 inhibited the aggregation of mHtt. Scale bar = 50 μm. Values are mean ± SEM (n = 3 or 4). $^{\$\$}P < 0.01$ versus control group (Student's t-test), $^{**}P < 0.01$ versus vehicle group (Student's t-test), $^{\#\#}P < 0.01$ versus vehicle group (Student's t-test). mHtt, mutant huntingtin.

induced by SUN N8075 6 h after treatment (Fig. 5A). Importantly, the expression level of *Vgf* mRNA expression level was not changed by U0126 treatment alone. Thus, the protective effect of SUN N8075 in STHdhQ111 cells was significantly decreased by treatment with U0126 and PD184352 (Fig. 5B and C).

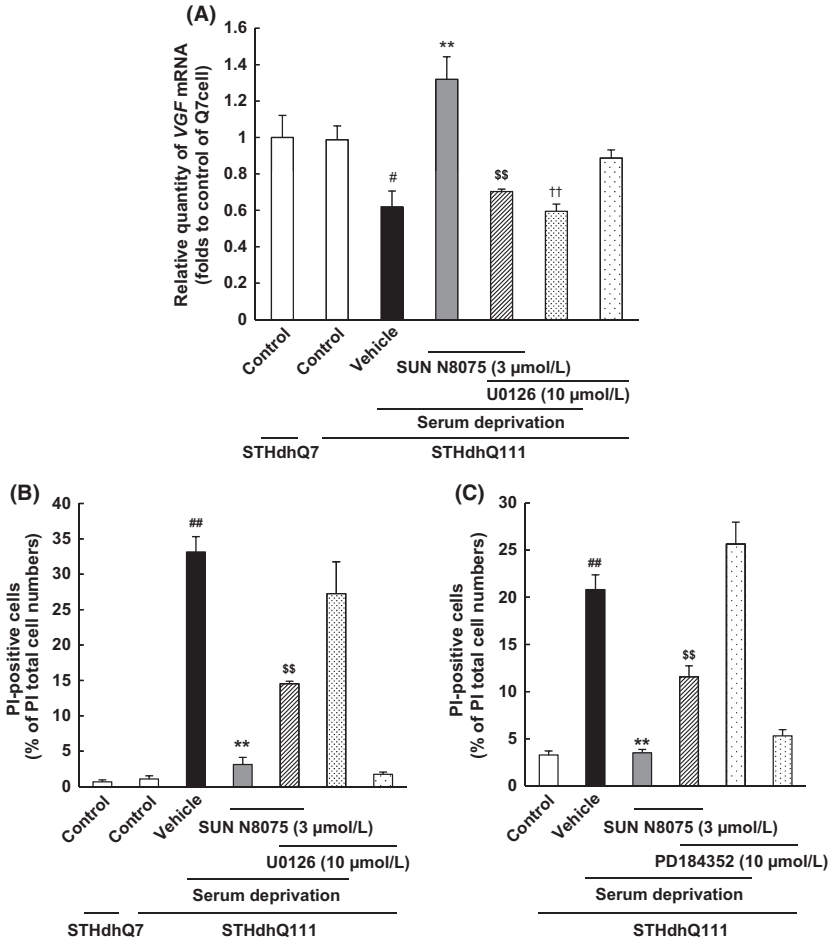

Figure 5. MEK inhibition suppressed the upregulation of *Vgf* mRNA and neuroprotective effects which are induced by SUN N8075. (A) The graph shows the relative quantity of *Vgf* mRNA (folds to control of STHdhQ7 cells). U0126 (10 μmol/L) suppressed the upregulation of *Vgf* mRNA expression induced by SUN N8075 6 h after treatment. Values are mean ± SEM ($n = 4$). $^{\#}P < 0.05$ versus control group for STHdhQ111 cells (Tukey's test), $^{**}P < 0.01$ versus vehicle group in STHdhQ111 (Tukey's test), $^{\$\$}P < 0.01$ versus SUN N8075-treated group in STHdhQ111 (Tukey's test), $^{\dagger\dagger}P < 0.01$ versus U0126-treated group which was not serum free in STHdhQ111 cells (Tukey's test). (B, C) The number of cells exhibiting PI fluorescence was counted, and positive cells were expressed as the percentage of PI-positive to Hoechst 33342-positive cells. (B) U0126suppressed the neuroprotective effects of SUN N8075. Values are mean ± SEM ($n = 4$). $^{\#\#}P < 0.01$ versus control group in STHdhQ111 (Tukey's test), $^{**}P < 0.01$ versus vehicle group in STHdhQ111 (Tukey's test), $^{\$\$}P < 0.01$ versus SUN N8075-treated group in STHdhQ111 cells (Tukey's test). (C) PD184352 suppressed the neuroprotective effects of SUN N8075. Values are mean ± SEM ($n = 4$). $^{\#\#}P < 0.01$ versus control group in STHdhQ111 (Tukey's test), $^{**}P < 0.01$ versus vehicle group in STHdhQ111 (Tukey's test), $^{\$\$}P < 0.01$ versus SUN N8075-treated group in STHdhQ111 cells (Tukey's test). PI, propidium iodide; VGF, VGF nerve growth factor inducible.

SUN N8075 prolonged survival in R6/2 HD mice

In an in vitro study, it was confirmed that SUN N8075 inhibited cell death. Next, we evaluated the effects of SUN N8075 in vivo using the HD model animal (R6/2 mouse) for the 5′-end of the human *huntingtin* gene carrying (CAG)115-(CAG)150 repeat expansions. The treatment with SUN N8075 commenced when the R6/2 mice were 4 weeks of age. The effects of SUN N8075 on survival in R6/2 mice are shown in Figure 5. Treatment with SUN N8075 (30 mg/kg per day; s.c.) significantly prolonged the mean lifespan by 25.0% ($P = 0.014$) in the R6/2 mice compared to vehicle-treated R6/2 mice (Fig. 6A). There were no significant differences in body weight between SUN N8075-treated and vehicle-treated R6/2 mice at any age (Fig. 6B).

Motor dysfunction in SUN N8075-treated R6/2 HD mice

Hindlimb and forelimb clasping have been observed in transgenic lines in which there is motor dysfunction or degeneration, including HD mouse models expressing

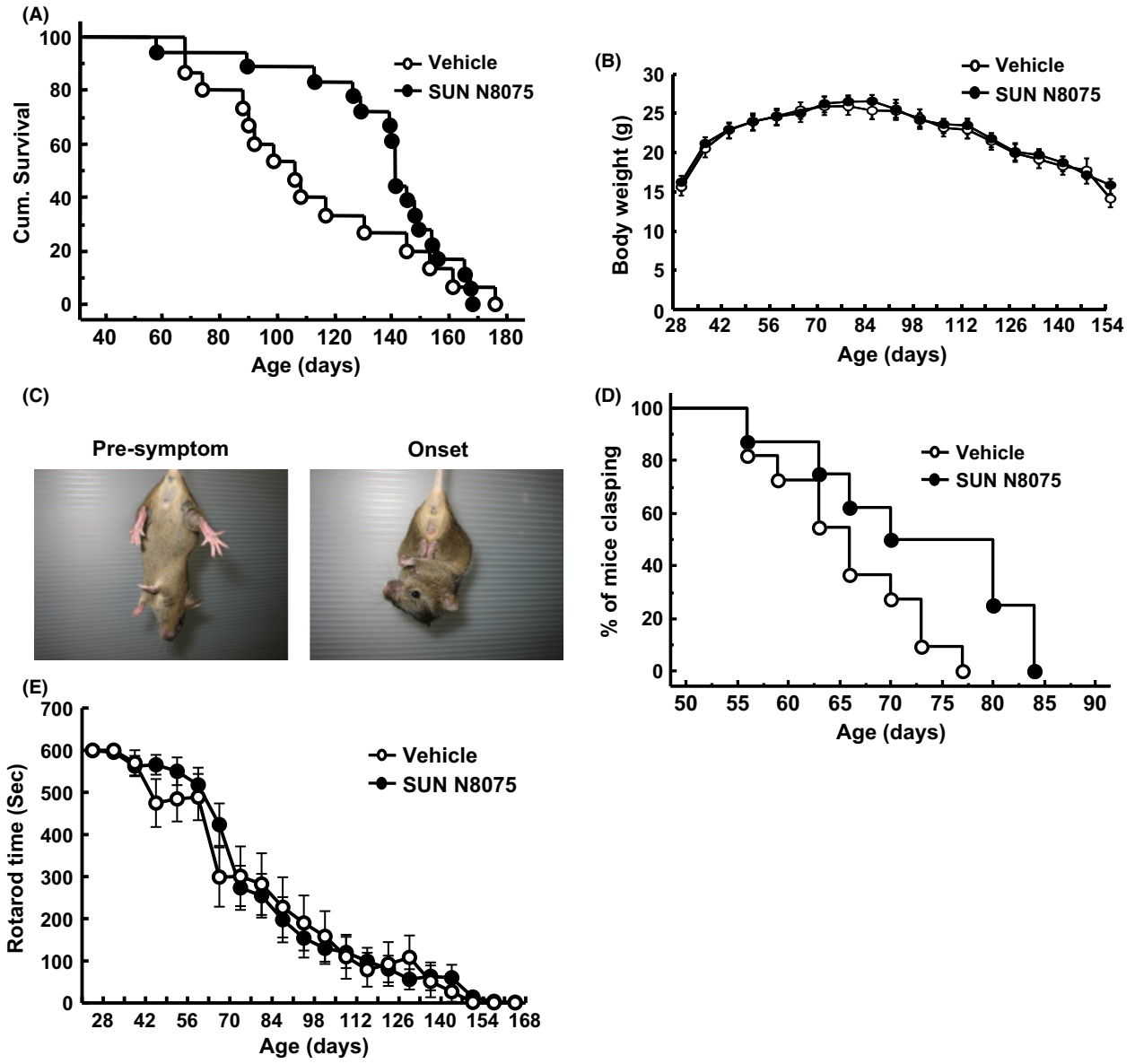

Figure 6. In vivo experiments to investigate the effects of SUN N8075 in R6/2 mice. (A) The effects of SUN N8075 at 30 mg/kg per day, s.c., on survival in R6/2 mice. The mean survival of vehicle-treated and the SUN N8075-treated mice were 109.3 ± 8.7 (n = 16) and 137.2 ± 6.5 (n = 18), respectively. (B) The body mass curves from R6/2 mice during treatment with SUN N8075 did not differ from those of the vehicle-treated mice. Values are means ± SEM (vehicle group, n = 16; SUN N8075 group, n = 18). (C) R6/2 mice at a presymptomatic age (age 8 weeks) and at the time of symptom onset (age 11 weeks). (D) Percentage of mice clasping in the vehicle-treated and SUN N8075-treated groups. Treatment with SUN N8075 significantly reduced the clasping phenotype in R6/2 mice. Values are means ± SEM (vehicle group, n = 11; SUN N8075 group, n = 8). (E) The effects of SUN N8075 at 30 mg/kg per day, s.c., on motor performance of R6/2 mice in the rotarod test. There were no significant differences between the vehicle-treated and SUN N8075-treated mice. Values are means ± SEM (vehicle group, n = 16; SUN N8075 group, n = 18).

mutant Htt (Auerbach et al. 2001; Guidetti et al. 2001). Additionally, HD model mice show a progressive decrease in retention times in the rotarod compared to age-matched wild-type littermate mice (Rodriguez-Lebron et al. 2005). We investigated the effects of SUN N8075 on the progression of these phenotypes by using the tail suspension and rotarod tests in R6/2 mice. Before disease onset, R6/2 mice often splay their legs out when suspended; however, the clasping response was observed at onset (Fig. 6C). Treatment with SUN N8075 (30 mg/kg per day; s.c.) significantly delayed onset of the clasping response. Kaplan–Meier life curves suggested that

treatment with SUN N8075 significantly increased survival ($P = 0.039$) in R6/2 mice (Fig. 6D). On the other hand, no significant differences were observed in motor performance in the rotarod test between SUN N8075-treated and vehicle-treated R6/2 mice (Fig. 6E).

SUN N8075 protected against neuronal cell death in R6/2 mice

We evaluated the effect of SUN N8075 on neuronal loss in the brains of R6/2 mice at 10 weeks of age. Representative photomicrographs of neuronal cells in the striatum are shown in Figure 7A–F. The high-magnification images of cresyl violet-stained brain sections (panels D wild type [WT], E [vehicle-treated group], and F [SUN N8075-treated group]) correspond with panels A, B, and C, respectively. Treatment with SUN N8075 (30 mg/kg per day; s.c.) significantly increased the number of surviving neurons compared with vehicle-treated R6/2 mice (Fig. 7G).

Discussion

In the present study, we demonstrated that SUN N8075 exerted neuroprotective effects in both in vitro and in vivo HD models. The efficacy of SUN N8075 was clearly indicated by the suppression of neuronal loss of striatum in the R6/2 mice. Furthermore, SUN N8075 upregulated *Vgf* mRNA expression via the phosphorylation of ERK1/2, resulting in suppression of cell death.

VGF is a secreted polypeptide that is expressed throughout the brain, especially in neurons, as well as in several endocrine and neuroendocrine that include the pancreas and pituitary and it regulates food intake and/or energy balance (Salton et al. 2000; Levi et al. 2004). Furthermore, the neuroprotective effects of VGF have been suggested to improve depression by enhancing hippocampal synaptic plasticity as well as neurogenesis in the dentate gyrus (Thakker-Varia et al. 2007). In the present study, SUN N8075 suppressed cell death (Fig. 1) and upregulated *Vgf* mRNA expression (Fig. 3A). Furthermore,

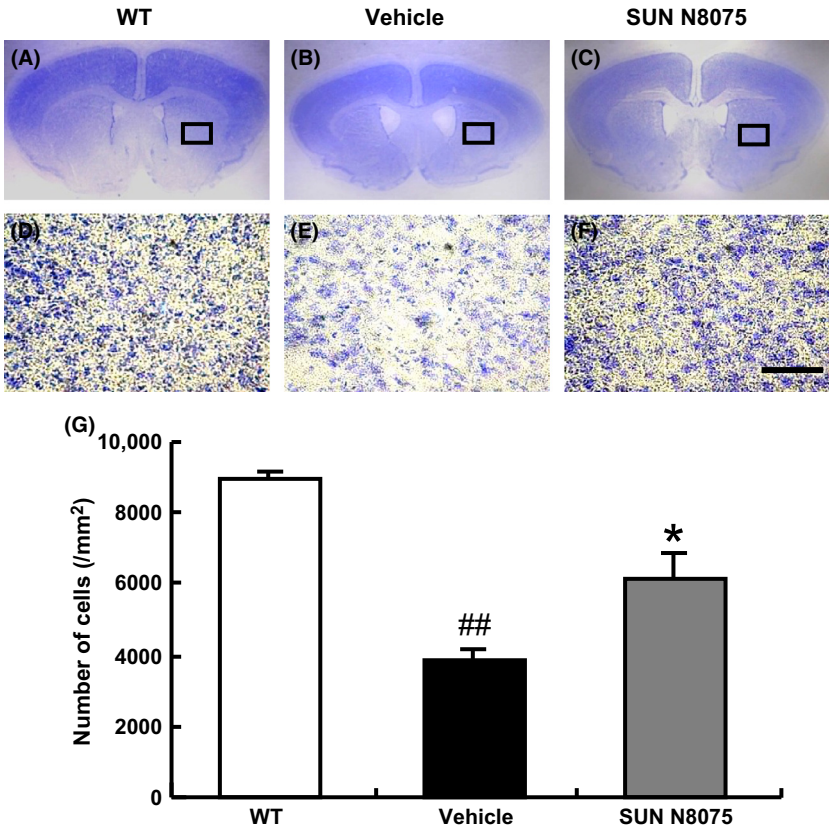

Figure 7. The effects of SUN N8075 on the decreasing numbers of striatal neurons in R6/2 mice. (A–F) Cresyl violet staining performed in coronal sections through the striatum of R6/2 mice; (A, D) wild-type (WT), (B, E) vehicle-treated mice, and (C, F) SUN N8075-treated mice. Scale bar = 50 μm. (G) The numbers of neurons in the striatum were significantly increased in SUN N8075-treated mice. Values are means ± SEM (WT, $n = 3$; Vehicle group, $n = 3$; SUN N8075 group, $n = 3$). $^{\#\#}P < 0.01$ versus WT mice (Student's *t*-test), $^{*}P < 0.05$ versus vehicle-treated mice (Student's *t*-test).

AQEE-30, which is well known as a VGF peptide, suppressed cell death, and the aggregation of mHtt in STHdhQ111 cells (Figs. 3C, 4); however, TLQP-21, another VGF peptide, did not exert a suppressive effect on STHdhQ111 cell death (Fig. 3D). In this study we have chosen two VGF peptides, AQEE-30 and TLQP-21. It is known that bioactive peptides are generated mainly by cleavage of VGF C-terminal. Because the sequence of AQEE-30 and TLQP-21 do not overlap, investigating these peptides may contribute to the greater understanding of the effects of VGF. These results indicate that SUN N8075 suppresses cell death via the upregulation of VGF expression and it inhibited the mHtt aggregation. In this study, we evaluated the mHtt aggregation as previously reported (Wang et al. 2011). It would have been useful to discriminate between the nuclear and cytosolic aggregate since nuclear aggregates have been reported as being more toxic to the cells (Davies et al. 1997), however, in STHdhQ111 cells, we were not able to determine the localization of mHtt because the expression of mHtt was not at a high enough level.

VGF is encoded by a gene that is responsive to brain-derived neurotrophic factor (BDNF) (Thakker-Varia et al. 2007) and is upregulated by BDNF through the MEK/ERK signaling pathway. We previously reported that SUN N8075 inhibited ER-stress-induced neuronal cell death via an increase in VGF expression and activation of the MEK/ERK pathway (Shimazawa et al. 2010). MEK/ERK signaling has been implicated in the hyperphosphorylation of Elk-1 and CREB, which are transcription factors induced by ERK activation; importantly, earlier studies have observed Elk-1 and CREB hyperphosphorylation in the striatum of R6/2 mice (Lievens et al. 2002; Obrietan and Hoyt 2004). Furthermore, several protein tyrosine phosphatases, which increase the dephosphorylation/inactivation of ERK1/2, were found to result in increased cell death in an HD model using PC12 cells such that the downregulation of p-ERK1/2 phosphorylation was correlated with the aggregation of mHtt (Wu et al. 2002). It has also been reported that the polyphenols fisetin and resveratrol provide neuroprotective effects via ERK activation in R6/2 mice (Maher et al. 2011). In the present study, ERK1/2 phosphorylation was induced 1 h after treatment with SUN N8075 (Fig. 2B–D). Furthermore, SUN N8075 increased the expression of *Vgf* mRNA 6 h after treatment, and this upregulation of *Vgf* mRNA was inhibited by an MEK inhibitor, thus attenuating the beneficial effects of SUN N8075 on cell death (Figs. 3, 5A–C). These results suggest that SUN N8075 exerts neuroprotective effects via activation of the MEK/ERK pathway.

In our in vivo study, SUN N8075 prolonged the mean lifespan of R6/2 mice by 25.0% compared with that of vehicle-treated R6/2 mice (Fig. 6A). In a previous study, various medicinal agents applied to R6/2 mice, such as riluzole, minocycline, and cystamine, prolonged the mean lifespan by only 10.2%, 14.0%, and 19.5%, respectively (Chen et al. 2000; Dedeoglu et al. 2002; Schiefer et al. 2002). These findings indicate that the therapeutic effect of SUN N8075 on survival is more potent than that of these previously tested compounds. Furthermore, treatment with SUN N8075 delayed the onset of clasping behavior (Fig. 6D) and inhibited neuronal cell death in the striatum of R6/2 mice (Fig. 7). We can speculate that SUN N8075 may have delayed onset of the clasping phenotype via the inhibition of neuronal cell death; however, further study will be required to elucidate the mechanisms of SUN N8075's effects in R6/2 mice.

In conclusion, we demonstrated that SUN N8075 inhibited cell death, via the upregulation of VGF expression and ERK 1/2 phosphorylation in STHdhQ111 cells. Additionally, treatment with SUN N8075 prolonged survival, delayed symptom onset, and inhibited the striatal neuronal cell death in the R6/2 mouse model of HD mice. SUN N8075 may be an important candidate compound for the treatment of HD and other neurodegenerative disorders.

Disclosure

S. T. and T. I. are employees of Asubio Pharma.

References

Adachi M, Barrot M, Autry AE, Theobald D, Monteggia LM (2008). Selective loss of brain-derived neurotrophic factor in the dentate gyrus attenuates antidepressant efficacy. Biol Psychiatry 63: 642–649.

Akane M, Shimazawa M, Inokuchi Y, Tsuruma K, Hara H (2011). SUN N8075, a novel radical scavenger, protects against retinal cell death in mice. Neurosci Lett 488: 87–91.

Annoura H, Nakanishi K, Toba T, Takemoto N, Imajo S, Miyajima A, et al. (2000). Discovery of (2S)-1-(4-amino-2,3,5-trimethylphenoxy)-3-[4-[4-(4- fluorobenzyl)phenyl]-1-piperazinyl]-2-propanol dimethanesulfonate (SUN N8075): a dual Na(+) and Ca(2 +) channel blocker with antioxidant activity. J Med Chem 43: 3372–3376.

Auerbach W, Hurlbert MS, Hilditch-Maguire P, Wadghiri YZ, Wheeler VC, Cohen SI, et al. (2001). The HD mutation causes progressive lethal neurological disease in mice expressing reduced levels of huntingtin. Hum Mol Genet 10: 2515–2523.

Baquet ZC, Gorski JA, Jones KR (2004). Early striatal dendrite deficits followed by neuron loss with advanced age in the absence of anterograde cortical brain-derived neurotrophic factor. J Neurosci 24: 4250–4258.

Browne SE, Bowling AC, Macgarvey U, Baik MJ, Berger SC, Muqit MM, et al. (1997). Oxidative damage and metabolic

dysfunction in Huntington's disease: selective vulnerability of the basal ganglia. Ann Neurol 41(5): 646–53.

Chen M, Ona VO, Li M, Ferrante RJ, Fink KB, Zhu S, et al. (2000). Minocycline inhibits caspase-1 and caspase-3 expression and delays mortality in a transgenic mouse model of Huntington disease. Nat Med 6: 797–801.

Davies SW, Turmaine M, Cozens BA, Difiglia M, Sharp AH, Ross CA, et al. (1997). Formation of neuronal intranuclear inclusions underlies the neurological dysfunction in mice transgenic for the HD mutation. Cell 90: 537–548.

Dedeoglu A, Kubilus JK, Jeitner TM, Matson SA, Bogdanov M, Kowall NW, et al. (2002). Therapeutic effects of cystamine in a murine model of Huntington's disease. J Neurosci 22: 8942–8950.

Duman RS, Monteggia LM (2006). A neurotrophic model for stress-related mood disorders. Biol Psychiatry 59: 1116–1127.

Guidetti P, Charles V, Chen EY, Reddy PH, Kordower JH, Whetsell WO Jr, et al. (2001). Early degenerative changes in transgenic mice expressing mutant huntingtin involve dendritic abnormalities but no impairment of mitochondrial energy production. Exp Neurol 169: 340–350.

Kotani Y, Morimoto N, Oida Y, Tamura Y, Tamura S, Inoue T, et al. (2007). Prevention of in vitro and in vivo acute ischemic neuronal damage by (2S)-1-(4-amino-2,3,5-trimethylphenoxy)-3-{4-[4-(4-fluorobenzyl) phenyl]-1-piperazinyl}-2-propanol dimethanesulfonate (SUN N8075), a novel neuroprotective agent with antioxidant properties. Neuroscience 149: 779–788.

Levi A, Ferri GL, Watson E, Possenti R, Salton SR (2004). Processing, distribution, and function of VGF, a neuronal and endocrine peptide precursor. Cell Mol Neurobiol 24: 517–533.

Lievens JC, Woodman B, Mahal A, Bates GP (2002). Abnormal phosphorylation of synapsin I predicts a neuronal transmission impairment in the R6/2 Huntington's disease transgenic mice. Mol Cell Neurosci 20: 638–648.

Maher P, Dargusch R, Bodai L, Gerard PE, Purcell JM, Marsh JL (2011). ERK activation by the polyphenols fisetin and resveratrol provides neuroprotection in multiple models of Huntington's disease. Hum Mol Genet 20: 261–270.

Mangiarini L, Sathasivam K, Seller M, Cozens B, Harper A, Hetherington C, et al. (1996). Exon 1 of the HD gene with an expanded CAG repeat is sufficient to cause a progressive neurological phenotype in transgenic mice. Cell 87: 493–506.

Monteggia LM, Barrot M, Powell CM, Berton O, Galanis V, Gemelli T, et al. (2004). Essential role of brain-derived neurotrophic factor in adult hippocampal function. Proc Natl Acad Sci USA 101: 10827–10832.

Obrietan K, Hoyt KR (2004). CRE-mediated transcription is increased in Huntington's disease transgenic mice. J Neurosci 24: 791–796.

Oyagi A, Oida Y, Hara H, Izuta H, Shimazawa M, Matsunaga N, et al. (2008). Protective effects of SUN N8075, a novel agent with antioxidant properties, in in vitro and in vivo models of Parkinson's disease. Brain Res 1214: 169–176.

Reijonen S, Putkonen N, Norremolle A, Lindholm D, Korhonen L (2008). Inhibition of endoplasmic reticulum stress counteracts neuronal cell death and protein aggregation caused by N-terminal mutant huntingtin proteins. Exp Cell Res 314 (5): 950–60.

Reiner A, Albin RL, Anderson KD, D'amato CJ, Penney JB, Young AB (1988). Differential loss of striatal projection neurons in Huntington disease. Proc Natl Acad Sci USA 85: 5733–5737.

Rodriguez-Lebron E, Denovan-Wright EM, Nash K, Lewin AS, Mandel RJ (2005). Intrastriatal rAAV-mediated delivery of anti-huntingtin shRNAs induces partial reversal of disease progression in R6/1 Huntington's disease transgenic mice. Mol Ther 12: 618–633.

Rubinsztein DC (2002). Lessons from animal models of Huntington's disease. Trends Genet 18: 202–209.

Salton SR, Ferri GL, Hahm S, Snyder SE, Wilson AJ, Possenti R, et al. (2000). VGF: a novel role for this neuronal and neuroendocrine polypeptide in the regulation of energy balance. Front Neuroendocrinol 21: 199–219.

Schiefer J, Landwehrmeyer GB, Luesse HG, Sprunken A, Puls C, Milkereit A, et al. (2002). Riluzole prolongs survival time and alters nuclear inclusion formation in a transgenic mouse model of Huntington's disease. Mov Disord 17: 748–757.

Shimazawa M, Tanaka H, Ito Y, Morimoto N, Tsuruma K, Kadokura M, et al. (2010). An inducer of VGF protects cells against ER stress-induced cell death and prolongs survival in the mutant SOD1 animal models of familial ALS. PLoS One 5: e15307.

Thakker-Varia S, Krol JJ, Nettleton J, Bilimoria PM, Bangasser DA, Shors TJ, et al. (2007). The neuropeptide VGF produces antidepressant-like behavioral effects and enhances proliferation in the hippocampus. J Neurosci 27: 12156–12167.

Wang Q, Liang G, Yang H, Wang S, Eckenhoff MF, Wei H (2011). The common inhaled anesthetic isoflurane increases aggregation of huntingtin and alters calcium homeostasis in a cell model of Huntington's disease. Toxicol Appl Pharmacol 250: 291–298.

Wu ZL, O'kane TM, Scott RW, Savage MJ, Bozyczko-Coyne D (2002). Protein tyrosine phosphatases are up-regulated and participate in cell death induced by polyglutamine expansion. J Biol Chem 277: 44208–44213.

Zuccato C, Ciammola A, Rigamonti D, Leavitt BR, Goffredo D, Conti L, et al. (2001). Loss of huntingtin-mediated BDNF gene transcription in Huntington's disease. Science 293: 493–498.